Advances in Science, Technology and Engineering Systems Journal Vol. 6, No. 4, 334-340 (2021)

www.astesj.com

ASTESJ

ISSN: 2415-6698

Theoretical study for Laser Lines in Carbon like Zn (XXV)

Nahed Hosny Wahba[*,1], Wessameldin Salah Abdelaziz[1], Tharwat Mahmoud Alshirbeni[2]

[1]Department of Laser Applications in Metrology, Photochemistry, and Agriculture, National Institute of Laser Enhanced Sciences, Cairo University, Giza, 12613, Egypt

[2]Physics Department, Faculty of Science, Cairo University, Giza 12613, Egypt

A R T I C L E I N F O

Article history:
Received: 06 July, 2021
Accepted: 08 August, 2021
Online: 16 August, 2021

Keywords:
FAC
C-like Zn (XXV)
Coupled Rate Equation
Reduced Population
Radiative Decay
Doppler Broadening Equation
Gain Coefficient

A B S T R A C T

The energy states, transitions chances, oscillator intensities, and collision intensities were computed with FAC (fully relativistic flexible atomic code) program. The calculated results were utilized for identification of the reduced population to sixty-nine thin structural states in C-like Zn (XXV) and indicates the gain coefficients with several electron densities (from 10^{+20} to 10^{+22} cm^3) and at a wide range of electron plasma temperatures (700,800,900,1000, &1100,1200,1300,1400,1500) eV. By using coupled rate equation to calculate the reduced population at different temperature and plotting that against electron densities; gives that at lower electron densities the reduced population proportional with reduced population till radiative decay happening; while at higher electron densities than 10^{+20} the radiative decay may be neglected in comparing with collisional depopulation so population states becomes independent and approximately the same. The gain coefficient was calculated by using the Doppler broadening equation of several transitions in Zn(XXV); these data plotted against electron density, and it was found that the gain was increased with temperature and producing the short wavelength laser , between 22 and 50 nm for the Zn^{30+}ion. The data was compared with the experimental calculations values collected by NIST and with the theoretical calculations of Bhatia, Seely & Feldman; where the calculated data differs from energy levels of Zn (XXV) comparing to experimental values in NIST at $(2p_{1/2}\,2p_{3/2})_1$ and $(2p_{1/2}\,2p_{3/2})_2$ by 0.05 and 0.04 successively; and it differs than the theoretical work of Bhatia at $(2p_{1/2}\,2p_{3/2})_1$ and $(2p_{1/2}\,2p_{3/2})_2$ by 0.05 Ryd and 0.04 Ryd successively also; which proved that our calculations are in well agreement with other works.

1. Introduction

X-ray lasers are a class of lasers in which gain has been demonstrated over various discrete wavelengths ranging from 3.56nm to 46.9nm. Because of the very short-duration and high-energy excitation pulses required to generate these lasers [1], [2], photo excitation method [3], Electron collisional pumping method (ECP), charge transfer technique, electron collisional recombination process and dielectronic recombination pumping are examples of X-ray pumping procedures which using picoseconds chirped pulse amplification (CPA) pulses [4]-[6]. Globally it's often observed that carbon is abundant element in astrophysical sits having the atmosphere. Emission lines of C-like ions are functionalized at prosopopoeia of the solar, astrophysical and melting plasmas whose illustrating needed exact atomic calculations; where the soft X-ray and XUV regions most of the data was found[7], [8]; thus Electron Collisional Pumping was functionalized to generate soft X-ray lasers after pumping methods[9], [10].

The process of pumping was illustrated as following:

$$X_l^{n+} + e \longrightarrow X_u^{n+}$$

where X_l^{n+} is a n-frequencies of atom ionization of the element X that pumping occurrence from lower level "l" to an excited level "u" in the same element atoms.

Theoretically there are more works done for computing the energy states, transition possibilities' and oscillator powers for Zn (XXV) [11]-[17]; while the gain for the same element not have

*Corresponding Author: Nahed Hosny Wahba, Department of Laser Applications in Metrology, Photochemistry, and Agriculture, National Institute of Laser Enhanced Sciences, Cairo University, Giza, 12613, Egypt
Email: nahedwahba77@gmail.com

https://dx.doi.org/10.25046/aj060437

more studies. The goal of this thesis is to utilize the atomic calculations such as energy states, oscillator powers and spontaneous radiative decay rates which calculated by using (FAC) program depending on Dirac equation for sixty nine thin-structure states to compute reduced populations and gain coefficients of C-like Zn excited states through a broad extent of electron densities (10^{+20} to10^{+23}) and at several electron temperatures (700, 800, 900, 1000, 1100, 1200, 1300, 1400 & 1500).These calculations might support the experimentalists for generating soft X-ray lasers.

2. Calculations equations used for Gain Coefficient determination

To calculate gain coefficient firstly energy levels, weighted oscillator strength and radiative rate for allowed transitions should be calculated; then the reduced population should calculated by solving coupled rate equation [18], [19]. After calculating the reduced population, it used to solve the Doppler broadening equation to obtain the gain coefficient.

Laser emission from Zn (XXV) ions plasma was investigated by studying the relation between several plasma temperatures and electron densities.

According to equation (1)

$$N_u\left[\sum_{l<u} A_{ul} + N_e\left(\sum_{l<u} C_{ul}^{d} + \sum_{l>u} C_{ul}^{e}\right)\right] = N_e\left(\sum_{l<u} N_l\, C_{lu}^{e} + \sum_{l>u} N_l\, C_{lu}^{d}\right) + \sum_{l>u} N_l\, A_{lu} \quad (1)$$

Since N_u and N_l are the fractional populations of levels u and l successively, A_{ul} represents Einstein coefficient for spontaneous radiative decay from u to l; N_e represents the electron density and C_{lu}^{e} $and C_{ul}^{d}$ are the rate coefficients for collisional excitation and de-excitation successively. The actual population density N_u of the u^{th} state can be computed from relation (2) [20][21].

$$C_{ul}^{d} = C_{lu}^{e}\left[\frac{g_l}{g_u}\right]\exp\left[\frac{\Delta E_{ul}}{kT_e}\right] \quad (2)$$

Since g_l and g_u represents a statistical weights of lower and upper states, successively.

The electron impact excitation rates identified by the effective collision strengths γ_{ul}
[20]Where;

$$C_{ul}^{d} = \frac{8.6287 * 10^{-6}}{g_u T_e^{1/2}}\gamma_{lu} \quad (3)$$

The measured population density N_u of the u^{th} was calculated [20],

$$N_U = N_u * N_l \quad (4)$$

Since $N_L$is the number of ions which achieved at the ionization stage L [20],

$$N_L = f_L\, {}^{N_e}\!/_{Z_{avg}} \quad (5)$$

Since N_e is the electron density, Z_{avg} is the average degree of ionization and f_L is the fractional abundance of the ionization levels were calculated [20]. Where the populations computed from Equation (1) is equal the unit;

$$\sum_{U=1}^{69}\frac{N_u}{N_l} = 1 \quad (6)$$

where the populations density calculated by Equation (1) is equal unit,

By computation the state's population density, the values N_u/g_u and N_l/g_l can be determined.

To prove that when inversion factor (F>0) gives positive gain equation (7) was used[22];

$$F = \frac{g_u}{N_u}\left[\frac{N_u}{g_u} - \frac{N_l}{g_l}\right] \quad (7)$$

Since N_u/g_u andN_l/g_l are the reduced populations of the upper state and lower state successively. Then Eq. (7) used to compute the gain coefficient (α) for Doppler broadening of the various transitions in the Zn (XXV) ion.

$$\alpha_{ul} = \frac{\lambda_{lu}^{3}}{8\pi}\left[\frac{M}{2\pi K T_l}\right]^{1/2} A_{ul} N_u\, F \quad (8)$$

Since M is the ion mass, $\lambda_{lu}$is the transition wavelength in (nm), and $T_l$is the ion temperature in eV.

3. Results and discussions

3.1. Energy states

With utilizing (FAC) [23] energy state measures for the $1s^2$ $2s^2$ 2pnl (n=3, l=s, p & d) and ml (m=4,l=s, p, d &f) configurations in C-like Zn^{+30} was obtained, this data presented in Tables (1); which shows the 69 energy levels of transition configurations:

Table (2) presented the comparison between our calculations of energy levels for Zn (XXV) the theoretical calculations by Bhatia, Seely and Feldman [12] and the actual results computed by NIST [24].

In table (2), the calculated data for energy levels of Zn (XXV) comparing to experimental values in NIST at $(2p_{1/2}\ 2p_{3/2})_1$ and $(2p_{1/2}\ 2p_{3/2})_2$ by 0.05 and 0.04 successively; and it differs than the theoretical work of Bhatia at $(2p_{1/2}\ 2p_{3/2})_1$ and $(2p_{1/2}\ 2p_{3/2})_2$ by 0.05 Ryd and 0.04 Ryd successively also; which proved that our calculations are in well agreement with other works.

3.2. Level population

Where increasing the excited electrons in higher energy states than in ground state causes the production of Laser in the XUV and soft X-ray spectral area;

Table 1: Energy states and definitions for Zn (XXV)

index	State configuration	Energy in (Ryd)*	Index	State configuration	Energy in (Ryd)*
1	$(2p_0)_0$	0	36	$(2p_{1/2}\,4p_{3/2})_2$	133.053
2	$(2p_{1/2}\,2p_{3/2})_1$	1.3831	37	$(2p_{1/2}\,4p_{1/2})_0$	133.075
3	$(2p_{1/2}\,2p_{3/2})_2$	1.9445	38	$(2p_{1/2}\,4s_{1/2})_2$	133.754
4	$(2p_2)_2$	3.8985	39	$(2p_{3/2}\,4s_{1/2})_1$	133.886
5	$(2p_0)_0$	5.6409	40	$(2p_{1/2}\,4d_{3/2})_2$	133.979
6	$(2p_{1/2}\,3s_{1/2})_0$	97.617	41	$2p_{1/2}\,4d_{5/2})_2$	133.994
7	$(2p_{1/2}\,3s_{1/2})_1$	97.715	42	$(2p_{1/2}\,4d_{5/2})_3$	134.003
8	$(2p_{3/2}\,3s_{1/2})_2$	99.576	43	$(2p_{1/2}\,4d_{3/2})_1$	134.016
9	$(2p_{3/2}\,3s_{1/2})_1$	99.657	44	$(2p_{3/2}\,4p_{1/2})_1$	134.400
10	$(2p_{1/2}\,3p_{1/2})_1$	99.907	45	$(2p_{3/2}\,4p_{3/2})_3$	134.424
11	$(2p_{1/2}\,3p_{3/2})_2$	100.488	46	$(2p_{3/2}\,4p_{1/2})_2$	134.440
12	$(2p_{1/2}\,3p_{3/2})_1$	100.490	47	$(2p_{3/2}\,4p_{3/2})_1$	134.447
13	$(2p_{1/2}\,3p_{1/2})_0$	100.568	48	$(2p_{1/2}\,4f_{5/2})_3$	134.873
14	$(2p_{3/2}\,3p_{3/2})_1$	102.038	49	$(2p_{1/2}\,4f_{5/2})_2$	134.921
15	$(2p_{3/2}\,3p_{3/2})_3$	102.206	50	$(2p_{1/2}\,4f_{7/2})_3$	134.996
16	$(2p_{3/2}\,3p_{1/2})_1$	102.230	51	$(2p_{1/2}\,4f_{7/2})_4$	135.019
17	$(2p_{3/2}\,3p_{1/2})_2$	102.275	52	$(2p_{3/2}\,4p_{3/2})_2$	135.251
18	$(2p_{1/2}\,3d_{3/2})_2$	102.289	53	$(2p_{3/2}\,4p_{3/2})_0$	135.496
19	$(2p_{3/2}\,3p_{3/2})_2$	102.812	54	$(2p_{3/2}\,4d_{5/2})_4$	135.854
20	$(2p_{1/2}\,3d_{5/2})_3$	102.842	55	$(2p_{3/2}\,4d_{3/2})_2$	135.866
21	$(2p_{1/2}\,3d_{5/2})_2$	102.979	56	$(2p_{3/2}\,4d_{3/2})_3$	135.928
22	$(2p_{1/2}3d_{3/2})_1$	103.056	57	$(2p_{3/2}\,4d_{5/2})_2$	135.993
23	$(2p_{3/2}\,3p_{3/2})_0$	103.722	58	$(2p_{3/2}\,4d_{3/2})_1$	136.004
24	$(2p_{3/2}\,3d_{5/2})_4$	104.441	59	$(2p_{3/2}\,4d_{3/2})_0$	136.005
25	$(2p_{3/2}\,3d_{3/2})_2$	104.474	60	$(2p_{3/2}\,4d_{5/2})_3$	136.192
26	$(2p_{3/2}\,3d_{5/2})_3$	104.717	61	$(2p_{3/2}\,4d_{5/2})_1$	136.232
27	$(2p_{3/2}\,3d_{5/2})_2$	104.892	62	$(2p_{3/2}\,4f_{5/2})_1$	136.421
28	$(2p_{3/2}\,3d_{3/2})_1$	104.907	63	$(2p_{3/2}\,4f_{7/2})_4$	136.450
29	$(2p_{3/2}\,3d_{3/2})_0$	104.921	64	$(2p_{3/2}\,4f_{5/2})_2$	136.475
30	$(2p_{3/2}\,3d_{5/2})_3$	105.508	65	$(2f_{3/2}\,4f_{7/2})_3$	136.488
31	$(2p_{3/2}\,3d_{5/2})_1$	105.564	66	$(2p_{3/2}\,4f_{7/2})_5$	136.508
32	$(2p_{1/2}\,4s_{1/2})_0$	131.880	67	$(2p_{3/2}\,4f_{5/2})_4$	136.522
33	$(2p_{1/2}\,4s_{1/2})_1$	131.914	68	$(2p_{1/2}\,4f_{5/2})_1$	136.540
34	$(2p_{1/2}\,4p_{1/2})_1$	132.702	69	$(2p_{3/2}\,4f_{7/2})_2$	136.580
35	$(2p_{1/2}\,4p_{3/2})_1$	133.037			

* Ryd is Rydberg constant

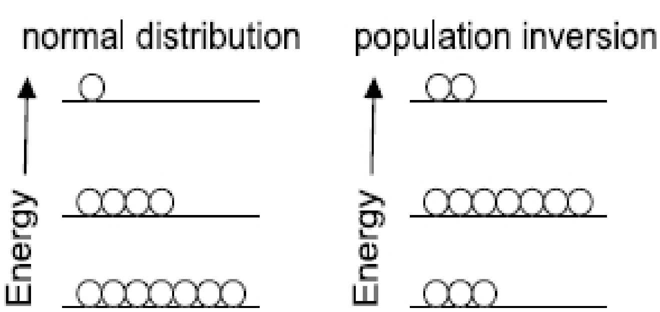

Schematic diagram of population inversion (Source of figure: https://spie.org/publications/fg08_p94_lasers?SSO=1)

index	State Configuration	Our calculation (FAC)(a)	S.S(b)	NIST(c)
1	$(2p_0)_0$	0	0	0
2	$(2p_{1/2}\,2p_{3/2})_1$	1.3831	1.4372	1.4370
3	$(2p_{1/2}\,2p_{3/2})_2$	1.9445	1.9866	1.9870
4	$(2p_2)_2$	3.8985	3.9122	...
5	$(2p_0)_0$	5.6409	5.3061	...
6	$(2p_{1/2}\,3s_{1/2})_0$	97.617	98.206	...
7	$(2p_{1/2}\,3s_{1/2})_1$	97.715	98.306	...
8	$(2p_{3/2}\,3s_{1/2})_2$	99.576	100.152	...
9	$(2p_{3/2}\,3s_{1/2})_1$	99.657	100.395	...
10	$(2p_{1/2}\,3p_{1/2})_1$	99.907	100.154	...
11	$(2p_{1/2}\,3p_{3/2})_2$	100.488	101.035	...
12	$(2p_{1/2}\,3p_{3/2})_1$	100.490	101.040	...
13	$(2p_{1/2}\,3p_{1/2})_0$	100.568	101.143	...
14	$(2p_{3/2}\,3p_{3/2})_1$	102.038	102.522	...
15	$(2p_{3/2}\,3p_{3/2})_3$	102.206	102.670	...
16	$(2p_{3/2}\,3p_{1/2})_1$	102.230	102.752	...
17	$(2p_{3/2}\,3p_{1/2})_2$	102.275	102.728	...
18	$(2p_{1/2}\,3d_{3/2})_2$	102.289	103.503	...
19	$(2p_{3/2}\,3p_{3/2})_2$	102.812	102.847	...
20	$(2p_{1/2}\,3d_{5/2})_3$	102.842	104.155	...
21	$(2p_{1/2}\,3d_{5/2})_2$	102.979	103.399	...
22	$(2p_{1/2}3d_{3/2})_1$	103.056	103.443	...
23	$(2p_{3/2}\,3p_{3/2})_0$	103.722	103.589	...
24	$(2p_{3/2}\,3d_{5/2})_4$	104.441	104.934	...
25	$(2p_{3/2}\,3d_{3/2})_2$	104.474	104.973	...
26	$(2p_{3/2}\,3d_{5/2})_3$	104.717	105.2[illegible]7	...
27	$(2p_{3/2}\,3d_{5/2})_2$	104.892	105.415	...
28	$(2p_{3/2}\,3d_{3/2})_1$	104.907	105.382	...
29	$(2p_{3/2}\,3d_{3/2})_0$	104.921	105.390	...

Thus the process of the reduced population densities was computed for sixty nine thin structure states starting from $1s^2\,2s^2$ 2pnl (n=3, l=s, p&d) and ml (m=4, l=s, p, d &f) configurations. The determination was done by applying the coupled rate Eq. (1) simultaneously using MATLAB version 7.10.0 (R2010a) computer program [25][17].

Figure (1 to 4) illustrate the reduced population for states $(2p_{3/2}3s_{1/2})_2$, $(2p_{1/2}3p_{3/2})_1$, $(2p_{3/2}3p_{3/2})_3$, $(2p_{3/2}3p_{3/2})_1$, $(2p_{3/2}3d_{5/2})_4$, and $(2p_{3/2}3d_{3/2})_3$at various temperatures (800,900,1000,1100)eV; so it can explain the behavior of states populations' density for several ions; where at low electron densities the reduced population densities are proportional to the electron densities, and the excitation process for an excited state is followed immediately by radiation decay. These results were agreed with the results of Feldman et.al. [11,17,24]. At electron density 10^{+19} various peaks were appeared; which means that radiative transitions dominant the de-excitation due its higher energy and fast decay time.

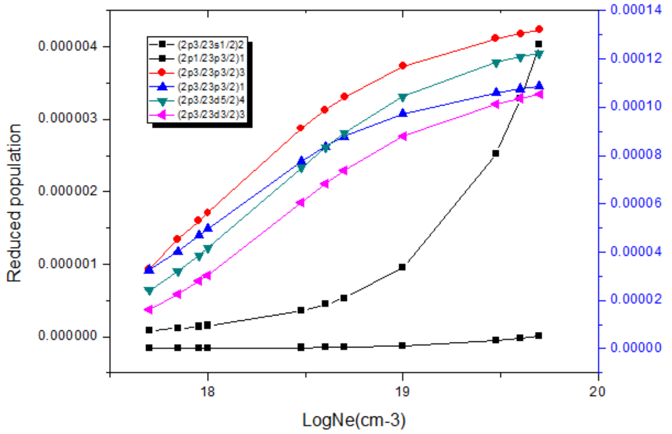

Figure 1: Reduced population of Zn^{+30} states at electron temperature 800eV.

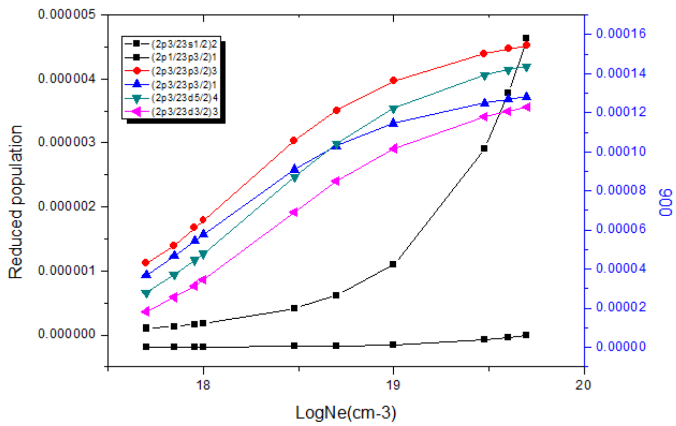

Figure 2: Reduced population of Zn^{+30} states at electron temperature 900eV.

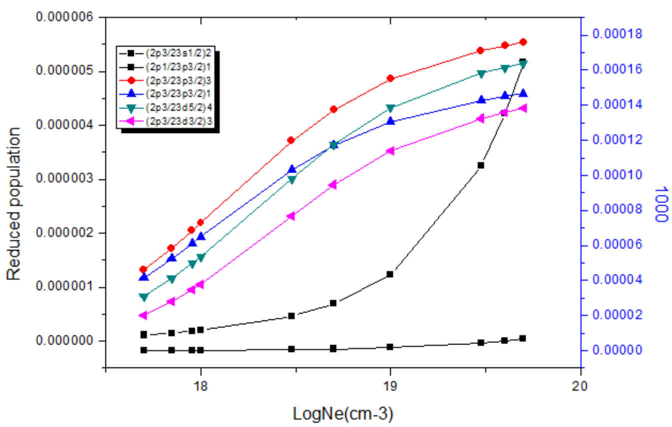

Figure 3: Reduced population of Zn^{+30} states at electron temperature 1000eV.

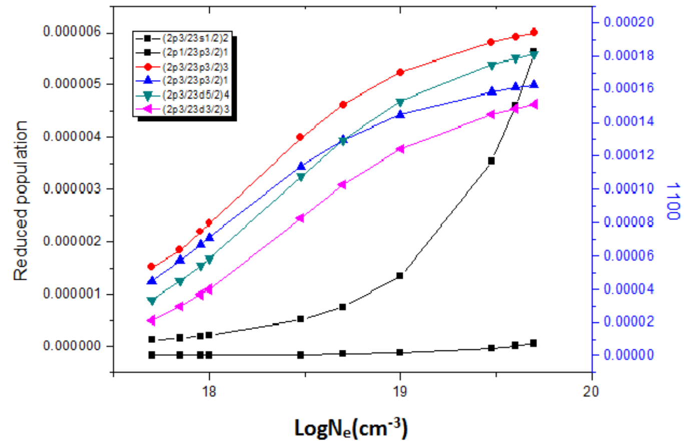

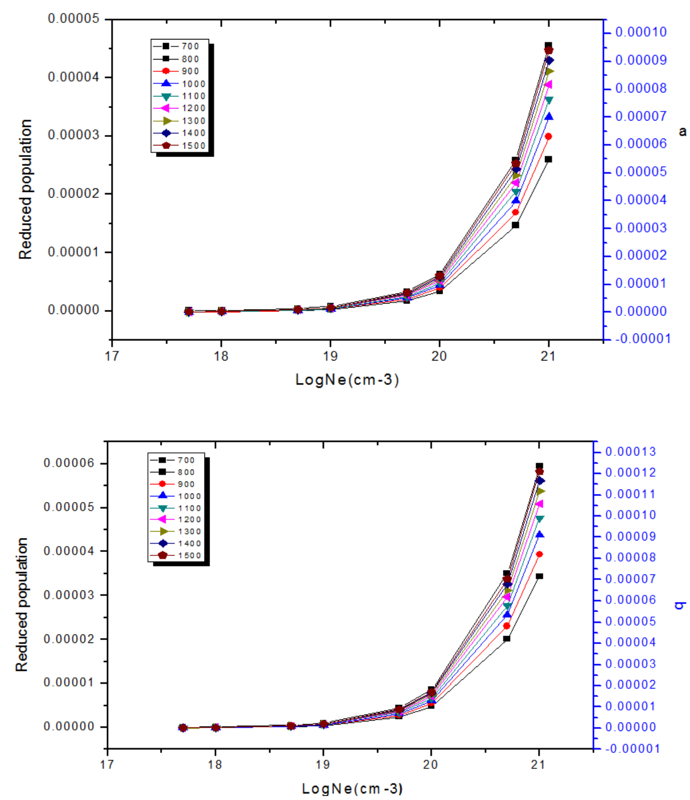

Figure 5: Reduced population of level (a) $(2p_{1/2}3p_{1/2})_1$, (b) $(2p_{1/2}3p_{3/2})_1$ for Zn (XXV) after electron collisional pumping as a function of the electron density at temperatures (700, 800, 900, 1000, 1100, 1200, 1300, 1400&1500) eV.

3.3. Radiative lifetime

atomic transfer probability is related to the life time u of an exited state

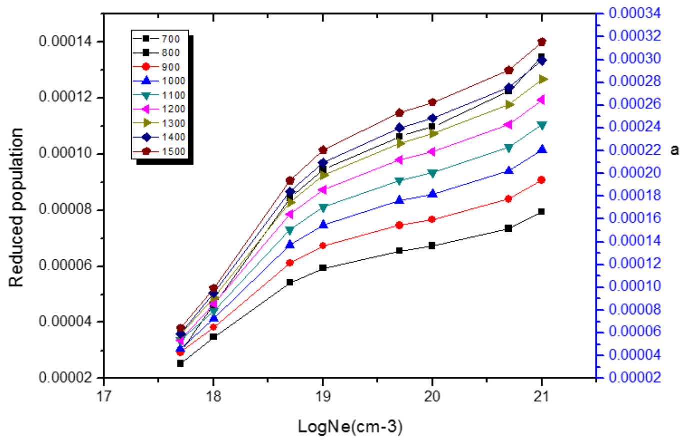

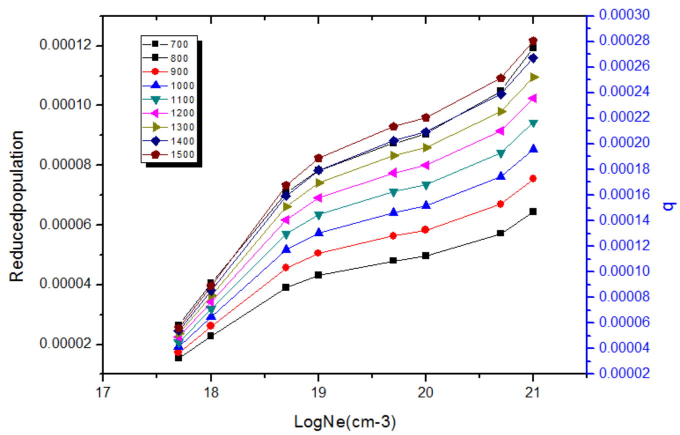

Figure 6: Reduced population of level (a) $(2p_{3/2}3p_{3/2})_3$, (b) $(2p_{3/2}3p_{3/2})_1$ for Zn (XXV) as a function of the electron density at different electron temperatures (700,800, 900, 1000, 1100, 1200, 1300, 1400&1500) eV.

$$\tau_u = \frac{1}{\sum_l A_{ul}} \tag{9}$$

Table 3. Illustrate the results of $(2p_{1/2}3d_{3/2})_2$--$(2p_{1/2}3p_{3/2})_1$, $(2p_{3/2}3d_{5/2})_4$—$(2p_{1/2}3p_{3/2})_1$and $(2p_{3/2}3d_{5/2})_4$—$((2p_{1/2}3p_{3/2})_2$radiative life time is longer than the lifetime of the lower state.

Configuration	τ_u(sec)	τ_l(sec)
$(2p_{3/2}3p_{3/2})_3$--$(2p_{1/2}3p_{1/2})_1$	8.926e-10	7.495e-10
$(2p_{1/2}3d_{3/2})_2$--$(2p_{1/2}3p_{3/2})_1$	9.894e-10	3.493e-12
$(2p_{3/2}3p_{3/2})_1$—$(2p_{1/2}3p_{3/2})_1$	2.578e-13	3.493e-12
$(2p_{3/2}3d_{5/2})_4$—$(2p_{1/2}3p_{3/2})_1$	2.104e-9	3.493e-12
$(2p_{3/2}3d_{5/2})_4$—$((2p_{1/2}3p_{3/2})_2$	2.104e-9	2.282e-10
$(2p_{3/2}3d_{3/2})_3$—$(2p_{1/2}3d_{3/2})_2$	5.597e-14	9.894e-10

3.4. Inversion factor

According to equation (7) the reduced population for lower states and upper states was calculated and demonstrate in the equation to calculate the inversion factor and it's found that the inversion factor is larger than zero. By using electron collisional pumping process the pumping quanta can be transferred to other state as a result of collision process, and this cause population inversion from the upper states to the lower states; whence this population inversion achieved appositive gain via F>0[21].

3.5. Gain coefficient

The gain process is the measure of the part of medium energy transferred to the emitted radiation which causes the amplification of the emitted radiation leading to strength optical power.

To calculate the gain the MATlab version the program was used to solve the coupled rate equation; this by using A_{ul} (spontaneous decay rates), C^e_{lu} (electron collisional excitation rate coefficients) and C^d_{ul} (electron collisional deexcitation rate coefficients).

$> 0.$

Finally the Doppler broadening equation was solved for various transitions to give the gain coefficient; then by plotting the relation between gain and electron density at different temperature to obtain the most intense laser transitions.

The figures (7, 8, 9, 10 & 11) illustrates the proportional relation between gain and electron density; and also have proportional relation between gain and temperature. According to the collected data it's found that the largest gain occur at temperature (1100eV) which give gain height of ($13.522 cm^{-1}$) at wavelength (50nm); this transition is at $(2p_{3/2}3p_{3/2})_1$—$(2p_{1/2}3p_{3/2})_1$ which refers to them by (16<>9). The smallest gain occur at temperature (800eV) which give gain height of ($2.5530cm^{-1}$) at wavelength (22.79nm); this gain transition at $(2p_{3/2}3d_{5/2})_4$—$(2p_{1/2}3p_{3/2})_1$which describe them as (22<>10); the gain of these transition at (22<>10) and at (16<>9) was plotted against electron densities at different temperatures. See Figure (11).

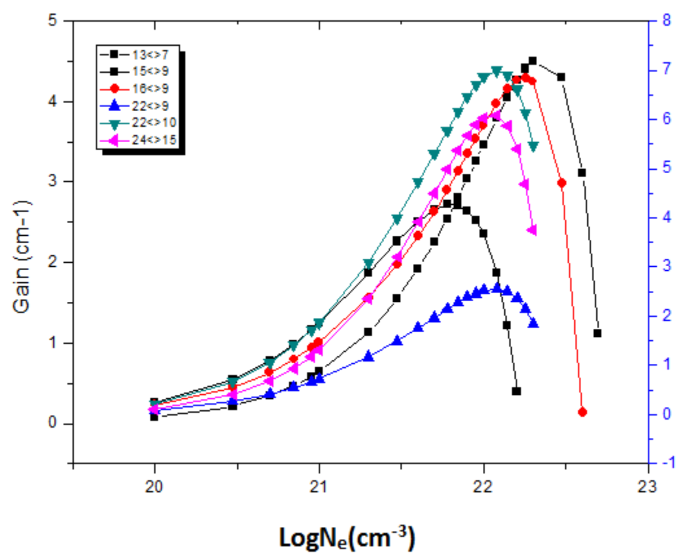

Figure 7: Electron density versus Gain coefficient at temperature 800 eV.

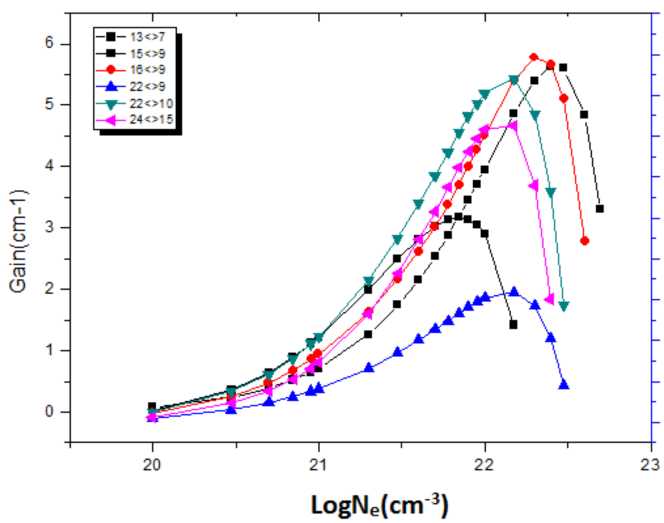

Figure 8: Electron density versus Gain coefficient at temperature 900 eV.

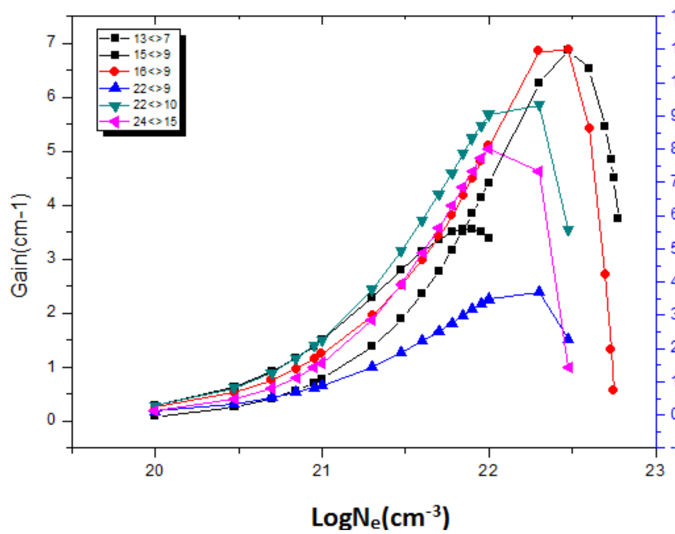

Figure 9: Electron density versus Gain coefficient at temperature1000 eV.

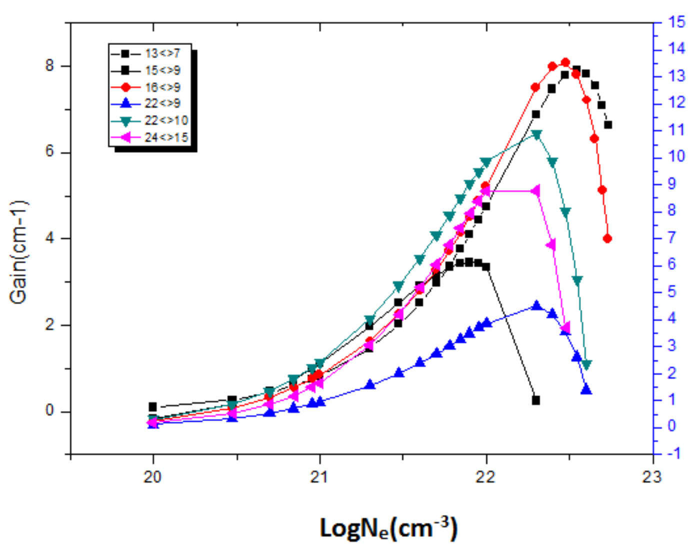

Figure 10: Electron density versus Gain coefficient at temperature1100 eV.

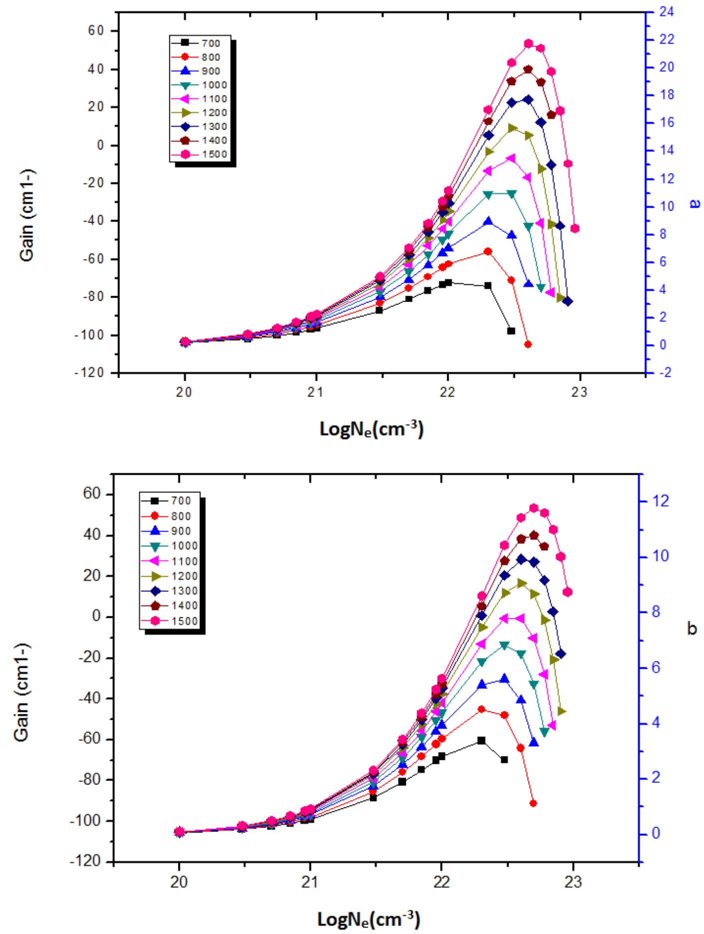

Table 4: configuration states, wavelength and maximum gain coefficient at various temperatures.

Configuration	λ(nm)	Gain(α)(cm⁻¹) Temperature eV								
		700	800	900	1000	1100	1200	1300	1400	1500
$(2p_{3/2}3p_{3/2})_3$--$(2p_{1/2}3p_{1/2})_1$	35.34	3.372	4.504	5.635	6.866	7.909	9.067	9.979	10.814	11.795
$(2p_{1/2}3d_{3/2})_2$--$(2p_{1/2}3p_{3/2})_1$	50.4	3.409	4.266	5.006	5.595	6.118	6.560	6.899	7.156	7.387
$(2p_{3/2}3p_{3/2})_1$—$(2p_{1/2}3p_{3/2})_1$	50	4.811	6.847	8.918	10.977	13.522	15.676	17.869	19.888	21.82
$(2p_{3/2}3d_{5/2})_4$—$(2p_{1/2}3p_{3/2})_1$	22.79	1.938	2.553	3.182	3.711	4.504	5.144	5.811	6.438	7.173
$(2p_{3/2}3d_{5/2})_4$—$(2p_{1/2}3p_{3/2})_2$	22.8	5.469	6.998	8.410	9.327	10.919	12.19	13.325	14.229	15.226
$(2p_{3/2}3d_{3/2})_3$—$(2p_{1/2}3d_{3/2})_2$	36.9	4.685	6.077	7.258	8.017	6.788	10.381	10.978	11.526	12.068

4. Conclusions

Conflict of Interest

The authors declare no conflict of interest.

Acknowledgment

The authors thanks both Prof. Dr. Souad ElFeky, Dr. Nagy Emara, and NILES their promotion and support.

References:

[1] William.T.Silfvast, Cambridge University press, second edi, 2000.
[2] B.N. Wellegehausen, B., Eichmann, H., Meyer, S., Momma, C., Mossavi, K., Welling, H., &Chichkov, "Generation of coherent VUV and XUV radiation. In ICONO'95: Fundamentals of Laser-Matter Interaction.," International Society for Optics and Photonics., **2796**, 132–139, 1996.
[3] A. Verma, R. Kumar, A. Parashar, "Enhanced thermal transport across a bi-crystalline graphene–polymer interface: an atomistic approach," Physical Chemistry Chemical Physics, **21**(11), 6229–6237, 2019. doi: 10.1039/C9CP00362B
[4] R.E. King, G.J. Pert, S.P. McCabe, P.A. Simms, A.G. MacPhee, C.L.S. Lewis, R. Keenan, R.M.N. O'Rourke, G.J. Tallents, S.J. Pestehe, "Saturated x-ray lasers at 196 and 73 Å pumped by a picosecond traveling-wave excitation," Physical Review A, **64**(5), 53810, 2001. doi: 10.1103/PhysRevA.64.053810
[5] A. V Vinogradov, I.I. Sobel'man, E.A. Yukov, "Population inversion of transitions in neon-like ions," Soviet Journal of Quantum Electronics, **7**(1), 32, 1977.
[6] B.A. Norton, N.J. Peacock, "Population inversion in laser-produced plasmas by pumping with opacity-broadened lines," Journal of Physics B: Atomic and Molecular Physics, **8**(6), 989, 1975.
[7] G. Tachiev, C.F. Fischer, "Breit-Pauli energy levels and transition rates for the carbonlike sequence," Canadian Journal of Physics, **79**(7), 955–976, 2001. doi: 10.1139/p01-059
[8] K.M. Aggarwal, F.P. Keenan, A.Z. Msezane, "Oscillator strengths for transitions in C-like ions between K XIV and Mn XX," Astronomy & Astrophysics, **401**(1), 377–383, 2003.
[9] V.A. Bhagavatula, "Soft x-ray population inversion by resonant photoexcitation in multicomponent laser plasmas," Journal of Applied Physics, **47**(10), 4535–4537, 1976.
[10] J. Nilsen, P. Beiersdorfer, S.R. Elliott, T.W. Phillips, B.A. Bryunetkin, V.M. Dyakin, T.A. Pikuz, A.Y. Faenov, S.A. Pikuz, S. Von Goeler, "Measurement of the Ly-α Mg resonance with the 2s→ 3p Ne-like Ge line," Physical Review A, **50**(3), 2143, 1994.
[11] U. Feldman, G.A. Doschek, J.F. Seely, A.K. Bhatia, "Short wavelength laser calculations for electron pumping in Be I and BI isoelectronic sequences (18≤ Z≤ 36)," Journal of Applied Physics, **58**(8), 2909–2915, 1985.
[12] A.K. Bhatia, J.F. Seely, U. Feldman, "Atomic data and spectral line intensities for the carbon isoelectronic sequence (Ar XIII through Kr XXXI)," Atomic Data and Nuclear Data Tables, **36**(3), 453–494, 1987, doi:https://doi.org/10.1016/0092-640X(87)90012-X.
[13] A. Verma, A. Parashar, "Molecular dynamics based simulations to study the fracture strength of monolayer graphene oxide," Nanotechnology, **29**(11), 115706, 2018, doi:10.1088/1361-6528/aaa8bb.
[14] A. Verma, A. Parashar, "Molecular dynamics based simulations to study failure morphology of hydroxyl and epoxide functionalised graphene," Computational Materials Science, **143**, 15–26, 2018.
[15] V. Singla, A. Verma, A. Parashar, "A molecular dynamics based study to estimate the point defects formation energies in graphene containing STW defects," Materials Research Express, **6**(1), 15606, 2018. doi: 10.1088/2053-1591
[16] A. Verma, A. Parashar, M. Packirisamy, "Atomistic modeling of graphene/hexagonal boron nitride polymer nanocomposites: a review," Wiley Interdisciplinary Reviews: Computational Molecular Science, **8**(3), e1346, 2018. doi: 10.1088/25192018
[17] U. Feldman, J.F. Seely, G.A. Doschek, A.K. Bhatia, "3 s–3 p laser gain and x-ray line ratios for the carbon isoelectronic sequence," Journal of Applied Physics, **59**(12), 3953–3957, 1986.
[18] U. Feldman, A.K. Bhatia, S. Suckewer, "Short wavelength laser calculations for electron pumping in neon-like krypton (Kr XXVII)," Journal of Applied Physics, **54**(5), 2188–2197, 1983.
[19] U. Feldman, J.F. Seely, A.K. Bhatia, "Scaling of collisionally pumped 3 s-3 p lasers in the neon isoelectronic sequence," Journal of Applied Physics, **56**(9), 2475–2478, 1984.
[20] W.H. Goldstein, J. Oreg, A. Zigler, A. Bar-Shalom, M. Klapisch, "Gain predictions for nickel-like gadolinium from a 181-level multiconfigurational distorted-wave collisional-radiative model," Physical Review A, **38**(4), 1797, 1988. doi: 10.1137/083627
[21] A. V Vinogradov, V.N. Shlyaptsev, "Calculations of population inversion due to transitions in multiply charged neon-like ions in the 200–2000 Å range," Soviet Journal of Quantum Electronics, **10**(6), 754, 1980.
[22] I.I.S. Man, Introduction to the theory of atomic spectra, International series of Monographs in Natural Philosophy, 40, Pergamon Press.
[23] [FAC Code. http://kipac-tree.stanford.edu/fac].
[24] NIST [http:///F:/NIST/NIST%20ASD%20Levels%20Output32.htm].
[25] R.D. Neidinger, "Introduction to automatic differentiation and MATLAB object-oriented programming," SIAM Review, **52**(3), 545–563, 2010. 10.1137/080743627